PAPER • OPEN ACCESS

Study of aerodynamics of the jet spreading over cylindrical surface

To cite this article: Zh K Seydulla et al 2019 J. Phys.: Conf. Ser. 1382 012038

View the <u>article online</u> for updates and enhancements.



IOP ebooks™

Bringing you innovative digital publishing with leading voices to create your essential collection of books in STEM research

Start exploring the collection - download the first chapter of every title for free.

1382 (2019) 012038 doi:10.1088/1742-6596/1382/1/012038

Study of aerodynamics of the jet spreading over cylindrical surface

Zh K Seydulla, M S Isataev and G K Toleuov

Kazakh National University Al-Farabi, Kazakhstan, Almaty

E-mail: seydulla92@mail.ru

Abstract. The purpose of this work is to study the fields of average values of velocity in a turbulent air jet propagating along a smooth cylindrical surface with an adjustable nozzle width being b, the curvature parameter SR and Re number on both convex and concave surfaces. To identify basic patterns of physical phenomena occurring in the boundary layer, it has been established that in universal coordinates, the wall velocity profiles have a universal nature in the region of a change in the curvature parameter $0 \le S_R \le |\pm 0.12|$, and virtually coincide with the velocity profiles of a turbulent boundary layer on a flat plate in a uniform flow past, except for the velocity peak region. This is due to the fact that the longitudinal pressure gradient is $104 \div 105$ times lower than transverse pressure gradient. According to our data, it has been established that the excess static pressure near the streamlined surface with a distance from the nozzle and an increase in jet thickness can reach up to 30–40% of the velocity head.

1. Experimental setup

A whole number of theoretical and experimental papers by various authors [1–11] are devoted to the study of the aerodynamics of near-wall jets propagating along a curvilinear surface. Currently, the study of near-wall jets extending along a smooth and rough curvilinear surface is of interest for practical application, as such jets are widely used in the internal combustion chambers of jet engines, combustion devices, aviation, construction of various types of facilities, etc.

In the existing works, the laws of aerodynamics were considered with a longitudinal jet flow around a flat plate and circular cylinder, for which the main flow patterns were discovered.

One of the varieties of semi-infinite flows is the jet flow around a cylindrical convex (concave) surface, which is a subject of sparse studies [4-6]. Some existing papers obtained approximate solutions to the problem of a near-wall laminar jet propagating along a convex cylindrical surface using small parameter expansion method, and there are some attempts to solve the problem for the turbulent jet [7, 8].

Experimental studies of the near-wall jet along a convex (concave) surface are also very few and do not demonstrate a complete picture of the flow. There are still no rigorous analytical calculations of near-wall turbulent jets due to the difficulty in combining calculations of the free boundary layer on the outer part of the jet with the boundary layer on the streamlined body surface. The task is even more complicated when considering a near-wall turbulent jet propagating along a convex or concave curvilinear surface. In this process, a transverse pressure gradient appears due to centrifugal inertial forces, which significantly affects the velocity profile in the jet sections, as well as the change in the maximum jet velocity and width with a distance from the nozzle.

Published under licence by IOP Publishing Ltd

Content from this work may be used under the terms of the Creative Commons Attribution 3.0 licence. Any further distribution of this work must maintain attribution to the author(s) and the title of the work, journal citation and DOI.

1382 (2019) 012038 doi:10.1088/1742-6596/1382/1/012038

Studying aerodynamics of a turbulent jet propagating along a curvilinear smooth and rough surface on both convex and concave surfaces allows approaching the theoretical solution of the problems related to near-wall turbulent flow, generalizing a large class of jet flow problems around different geometry surfaces.

The experimental setup for measuring the average velocity, static pressure and friction stress on the wall of a turbulent wall jet propagating along a concave or convex cylindrical surface is shown schematically in Figure 1.

The air jet, injected by fan 1, flowed out of the nozzle 4, with exit slit height h = 280mm and with adjustable width b from 5 mm to 40 mm. The streamlined cylindrical surface 5 with radius R = 360 mm is a continuation of one of the nozzle walls. The nozzle provided a uniform velocity profile at its output. To obtain a uniform and low-turbulent flow, honeycomb 2 and fine-meshed grids 3 were installed in front of it at the nozzle exit.

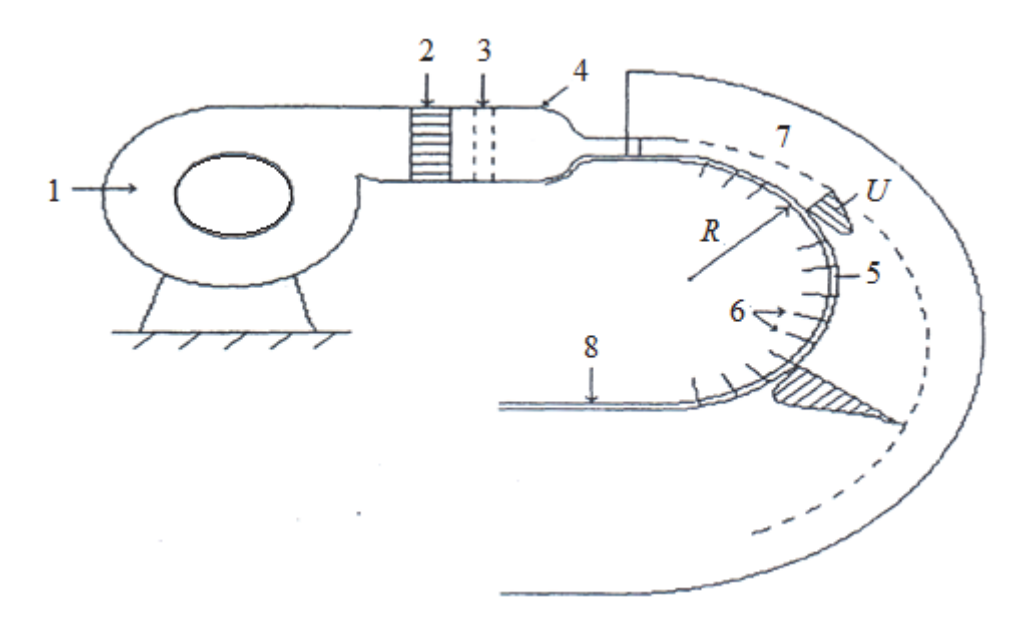


Figure 1. Experimental Unit Layout. 1 – fan, 2 – honeycomb, 3 – metal mesh, 4 – nozzle, 5 – cylindrical surface, 6 – drain holes, 7 – limiting side walls, 8 – flat extension.

The static pressure on the wall was measured using drain holes 6 with a diameter of 0.8 mm, drilled along the centerline of the nozzle slit height along the entire half-cylinder surface with a central angle from $\psi = 0$ to $\psi = 175^{\circ}$. To prevent the influence of the final cylinder height, the jet was limited to lateral flat walls 7. At the end of the cylindrical surface, a flat extension 8 was installed with a length of 300 mm to prevent the influence of end effects. The curvature parameter of the streamlined surface based on the initial width of the jet $S_R = b/R$ varied from +0.12 (convex surface) to -0.12 (concave surface).

The jet velocity was measured with a T-shaped nozzle with opposing openings. The nozzle was moved along the direction of the jet by the coordinate spacer with an accuracy of 1 mm, perpendicular to the body surface with an accuracy of 0.01 mm. The initial reading of the full-pressure tube position was determined by a break in its electrical contact with the metal surface of the working medium.

For a more accurate measurement of the velocity profile in the near-wall region, a Pitot tube with a flattened tip with external dimensions of $0.20 \text{ mm} \times 1.10 \text{ mm}$ was used.

The velocity was determined from the difference in the total pressure measured by a Pitot tube with a flattened tip and static pressure on the wall, measured using a drain hole on the wall.

For the study of aerodynamics, two halves of a steel cylinder with external radius R = 360 mm and internal radius R = 355 mm were used as a streamlined surface.

1382 (2019) 012038

doi:10.1088/1742-6596/1382/1/012038

Measurements of the velocity and static pressure profiles were taken in a jet propagating along a convex cylindrical surface with radius R = 360 mm at a nozzle outlet section width b = 5.0mm; 10.0 mm; 15.0 mm; 27.0 mm; 41.0 mm; and in a jet propagating along a concave cylindrical surface with radius R = 355 mm at a nozzle outlet section width b = 5.0 mm; 10.0 mm; 15.0 mm; 24.0 mm and 41 mm. Thus, the initial curvature parameter of the streamlined surface varied from $S_R = -0.117$ jet values along a concave surface to $S_R = 0.114$ for a jet along a convex surface.

Dynamic pressure and static pressure were measured with a T-shaped nozzle using the counter-tube method, and total pressure was measured with a Pitot tube. The static pressure distribution was also performed using the Prandtl tube for static pressure and the "washer" method. Static pressure distribution on the cylinder surface was measured through drain holes on the surface.

2. Results

Figures 2 and 3, for example, show dynamic and excess pressure profiles (compared to ambient pressure) of the static pressure, measured by a T-shaped nozzle, related to dynamic pressure of the initial velocity. In all experiments the jet was deployed along a cylindrical surface at an angle of 180°. In none of the cases of measurements, no boundary layer separation from the streamlined surface took place.

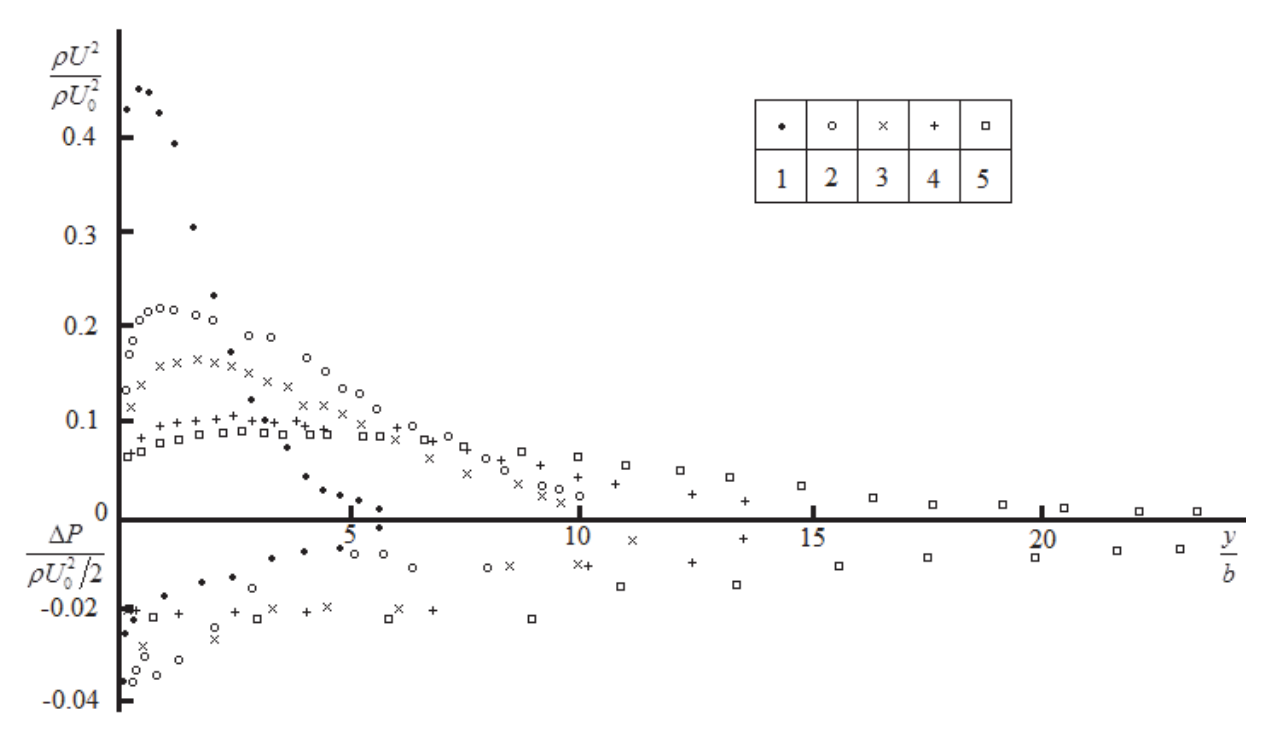


Figure 2. Head velocity profiles in a jet on a convex surface

$$U_0$$
=29.6 m/s; $1 - \frac{x}{b} = 25$; $2 - \frac{x}{b} = 50$; $3 - \frac{x}{b} = 61.4$; $4 - \frac{x}{b} = 83.4$; $5 - \frac{x}{b} = 134$.

From a comparison of the velocity profiles and static pressure for the convex and concave surfaces jet, it can be seen that the jet width expands and the maximum velocity decreases faster along the convex surface jet, compared to the concave surface jet; the excess static pressure in the convex surface jet is negative and on the concave surface it is positive near the surface. The static excess pressure decreases as the external boundary of the jet decreases in absolute value, but in both cases the excess static pressure becomes negative at the outer free boundary of the jet.

First of all, this is caused by the influence of the transverse jet velocity component, due to which the surrounding stationary medium is entrained by the jet. Secondly, due to the effect of the transverse

1382 (2019) 012038 doi:10

doi:10.1088/1742-6596/1382/1/012038

velocity component of the jet, the measuring nozzle tips are flown around obliquely and static pressure measurement error increases. Therefore, the static pressure measurement using the "washer" method on the outer part of the jet should be more accurate.

Figure 4 shows the static pressure profiles in the same jet section on a convex surface, measured in three ways: T-shaped nozzle, Prandtl static pressure tube, and using the "washer" method. As it can be seen, the first two nozzles render approximately the same values, whereas the "washer" method renders a much lower depression on the outer jet boundary, which is close to theoretical computation with regard to the transverse velocity component.

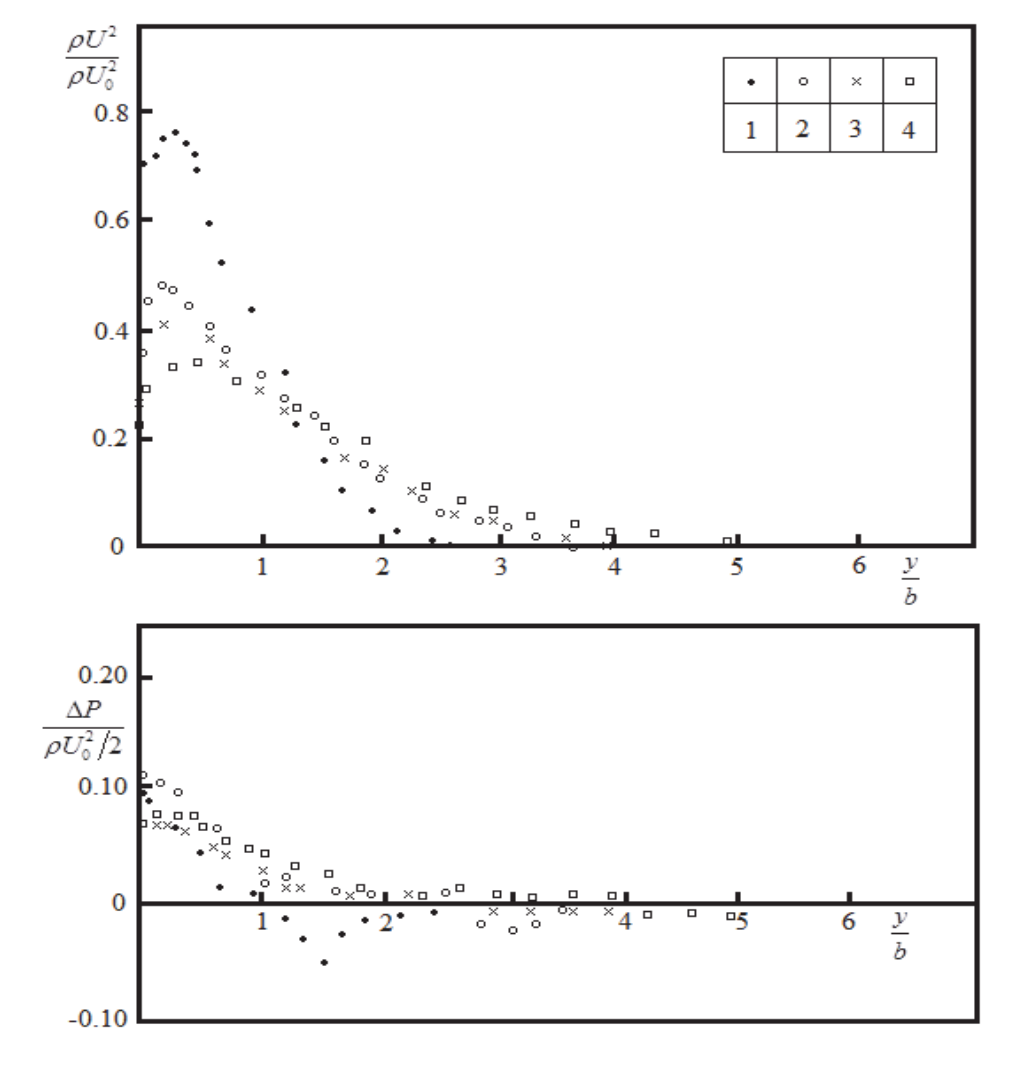


Figure 3. Profiles of velocity head and static pressure in a jet along a concave surface

$$U_0 = 29.6 \text{ m/s}; 1 - \frac{x}{h} = 15.3; 2 - \frac{x}{h} = 29.3; 3 - \frac{x}{h} = 37.0; 4 - \frac{x}{h} = 48.5.$$

The results of the static pressure measurement by the Prandtl tube and T-type nozzle are somewhat affected by the wall proximity in the near-wall region of the boundary layer, and it is impossible to measure this pressure close to the wall using the "washer" method. Therefore, the velocity profiles in the wall boundary layer were measured with a full-pressure flattened tip tube, taking into account the static pressure measured through the drain holes on the streamlined surface.

1382 (2019) 012038 doi:10.1088/1742-6596/1382/1/012038

Generally, the excess pressure in absolute value near the wall is the maximum and it drops gradually as it approaches the outer boundary of the jet.

The absolute value of the underpressure or overpressure, classified as initial dynamic pressure, varies only slightly with a distance from the nozzle and amounts to $2 \div 4\%$ of the initial velocity head. However, due to a decrease in the maximum velocity and an increase in the jet width with a distance from the nozzle, the underpressure in a jet on a convex surface and excessive pressure in a jet on a concave surface can reach a considerable value of up to 40% of the maximum velocity dynamic pressure. Therefore, when measuring the velocity fields, it is necessary to take into account the effect of static pressure on the readings of the measuring tips.

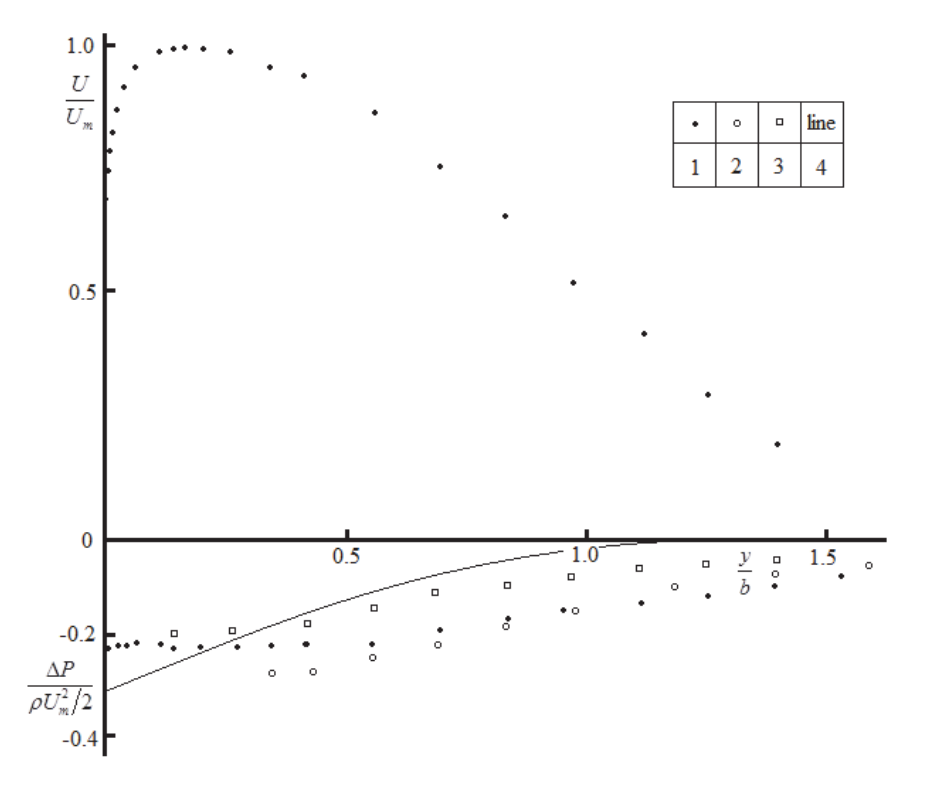


Figure 4. Speed and static pressure profiles measured by various nozzles 1-T-type nozzle; 2-P randtl static pressure tube; 3-u sing "washer" method; 4-b ased on the formula: $\frac{\Delta P}{\rho U_m^2/2} = \mp 1.4871 a \Big[1 \mp 0.4769 a + 0.3457 a^2 \mp 0.3141 a^3 \Big]$, where $a = \frac{\delta}{R} = S_R \times \frac{\delta}{b}$.

Figures 5 and 6 show the profiles of dimensionless velocity and static pressure for a jet on convex and concave surfaces in $\frac{U}{U_m} = f\left(\frac{y}{\delta}\right)$ and $\frac{\Delta P}{\rho U_m^2/2} = f\left(\frac{y}{\delta}\right)$ coordinates, where δ is the conventional jet width equal to the distance from the wall to the point where $U = \frac{U_m}{2}$ on the outer part of the profile, U_m is the maximum jet velocity in this section.

1382 (2019) 012038

doi:10.1088/1742-6596/1382/1/012038

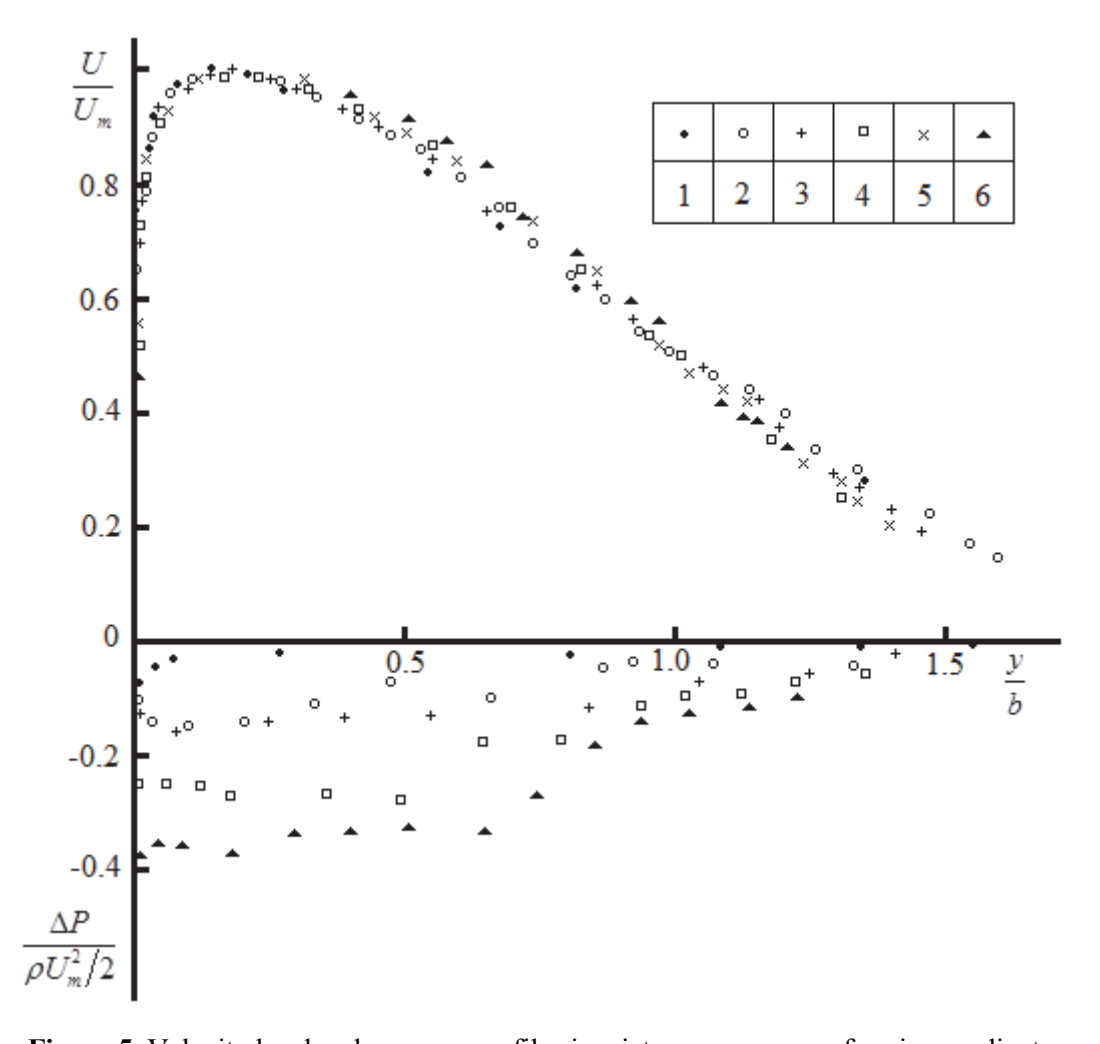


Figure 5. Velocity head and pressure profiles in a jet on a convex surface in coordinates

$$\frac{U}{U_m} = f\left(\frac{y}{\delta}\right), \ \frac{\Delta P}{\rho U_m^2/2} = f\left(\frac{y}{\delta}\right)$$

$$U_0 = 31.0 \text{ m/s}; \ 1 - \frac{x}{b} = 25; \ 2 - \frac{x}{b} = 50; \ 3 - \frac{x}{b} = 61.4; \ 4 - \frac{x}{b} = 83; \ 5 - \frac{x}{b} = 104; \ 6 - \frac{x}{b} = 134.$$

As it can be seen from the figures, the velocity profiles in coordinates $\frac{U}{U_m} = f\left(\frac{y}{\delta}\right)$ in all sections in the jet both along the convex and concave surfaces retain affinity, whereas static pressure distribution has no affinity. As we have shown based on analytical calculation, the pressure distribution $\frac{\Delta P}{\rho U_m^2/2}$

over the cross section depends not only on the initial curvature parameter $S_R = b/R$, but also on the current jet width δ/b , so there is no affinity of the dimensionless excess pressure profile. Non-dimension velocity profiles on a curvilinear surface do not almost differ from the velocity profiles of a near-wall jet propagating along a flat plate, which is satisfactorily described by the formula proposed by Professor S.I. Isataev

$$\frac{U}{U_m} = 1.426 \cdot \eta^{1/8} \left(1 - 0.503 \cdot \eta \right)^{3/2},\tag{1}$$

where $\eta = y/\delta$.

The influence of the pressure gradient on the wall velocity profile is interesting.

1382 (2019) 012038 doi:10.1088/1

8 doi:10.1088/1742-6596/1382/1/012038

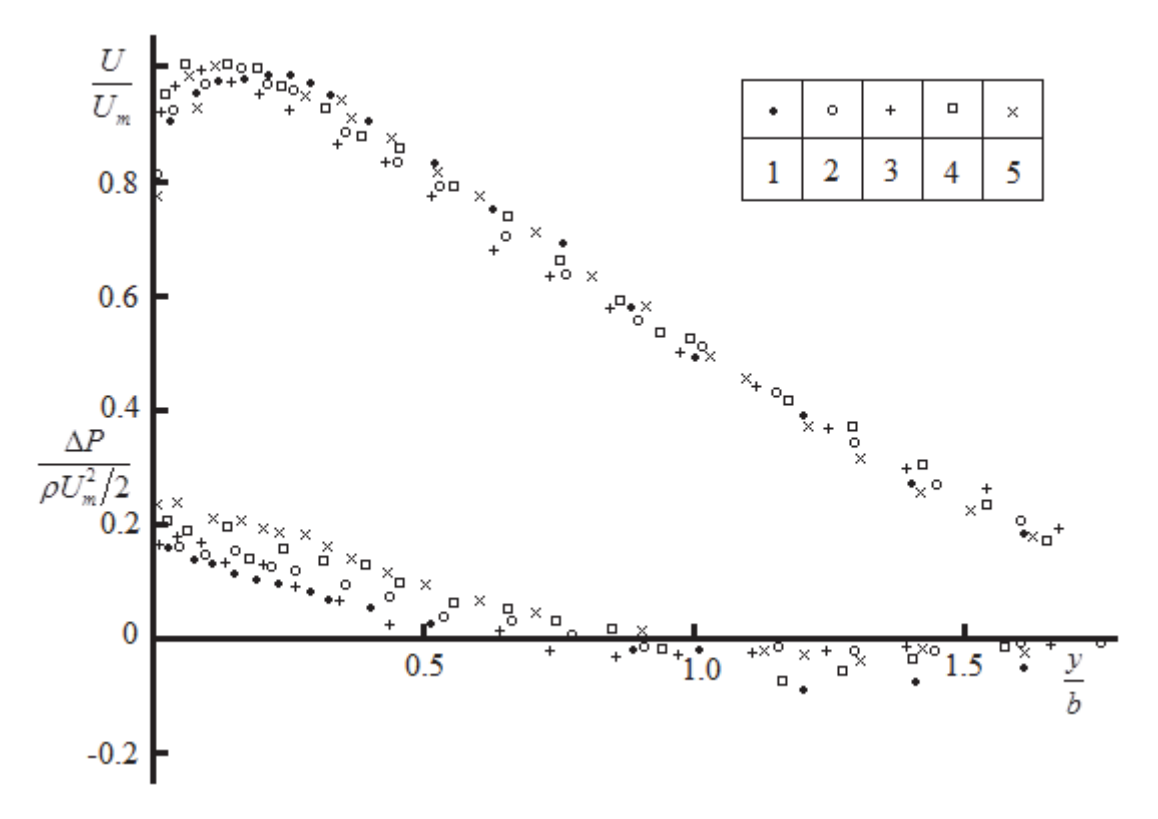


Figure 6. Profiles of velocity head and pressure in a jet on a concave surface

in coordinates
$$\frac{U}{U_m} = f\left(\frac{y}{\delta}\right)$$
, $\frac{\Delta P}{\rho U_m^2/2} = f\left(\frac{y}{\delta}\right)$
 $U_0 = 29.6 \text{ m/s}$; $1 - \frac{x}{b} = 21.3$; $2 - \frac{x}{b} = 36.9$; $3 - \frac{x}{b} = 42.2$; $4 - \frac{x}{b} = 48.5$; $5 - \frac{x}{b} = 55.4$.

As it is known, for a flat jet the ratio of the wall jet thickness to the conditional jet thickness, according to different authors, is in the interval of $0.14 \le \delta m/\delta \le 0.18$.

According to the formula (1)

$$\delta_m = 0.153\delta.$$
 (2)

Our experiments show that with increasing curvature of the streamlined surface and with a distance from the nozzle, the $\delta m/\delta$ ratio somewhat increases in the jet along the convex surface, and in the jet along the concave surface it tends to decrease. However, in view of the difficulty of accurately determining the wall jet thickness, this dependence is approximate.

Figures 7 and 8 are shown as an example of a change in the relative thickness of the wall boundary layer in the jet along convex and concave surfaces for different values of curvature parameter S_R . It can be seen that the relative thickness of the near-wall boundary layer varies very slightly with a distance from the nozzle and is almost independent of the initial curvature parameter S_R .

1382 (2019) 012038

doi:10.1088/1742-6596/1382/1/012038

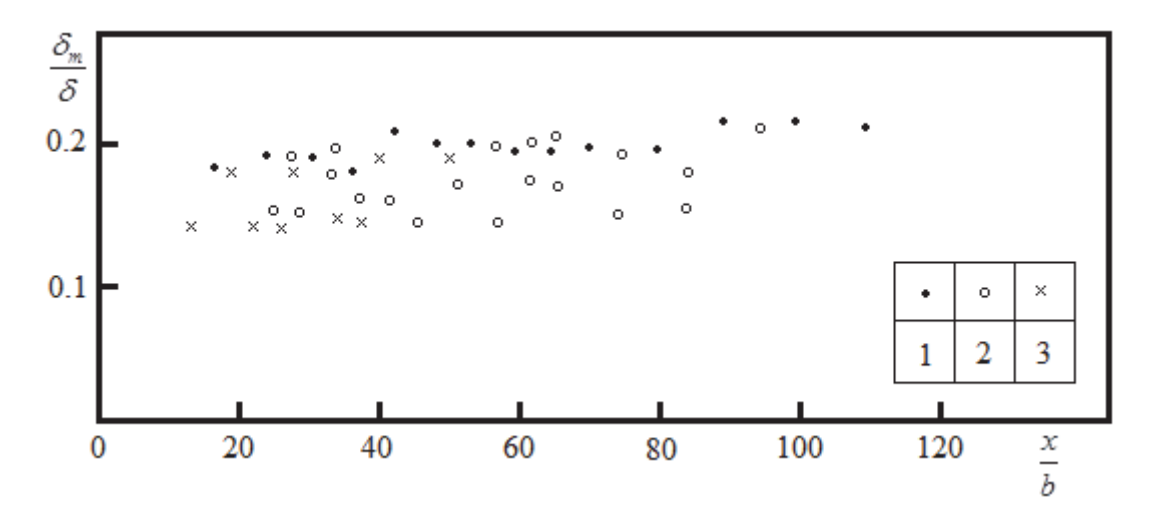


Figure 7. Change in the relative thickness of the wall boundary layer on a convex surface $1 - S_R = 0.014$; $2 - S_R = 0.028$; $3 - S_R = 0.042$.

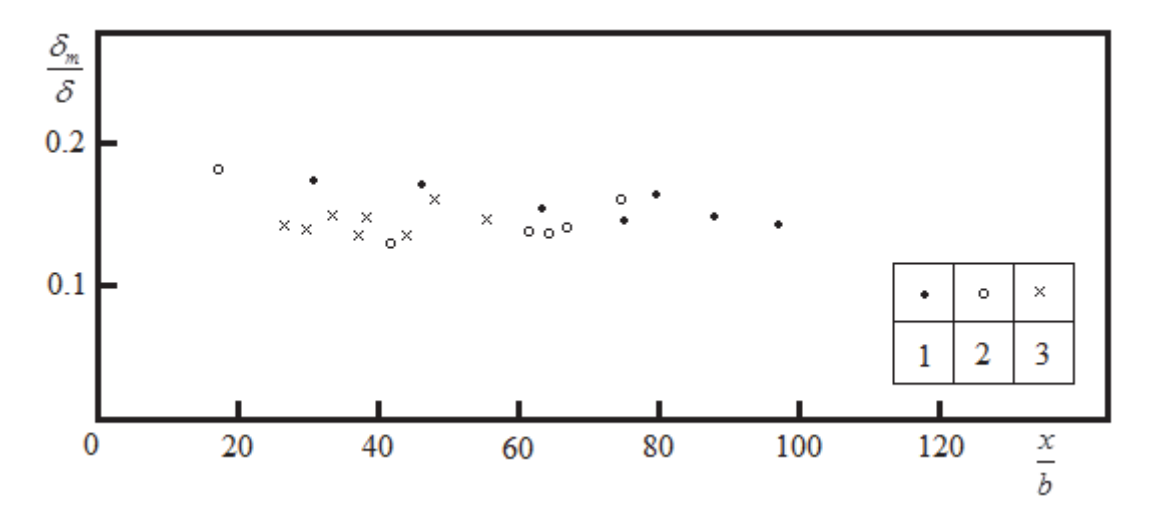


Figure 8. Changes in the thickness of the wall boundary layer in the jet along a concave surface $1 - S_R = 0.014$; $2 - S_R = 0.028$; $3 - S_R = 0.042$.

The velocity distribution in the near-wall boundary layer on a large scale is shown in Figures 9 and 10.

For comparison Figure 9 shows the velocity profiles in the jet propagating along the convex and concave surfaces, and Figure 10 shows the velocity profiles in the boundary layer of the jet along the concave surface for different sections for two values of the initial curvature parameter $S_R = 0.014$ and 0.042.

1382 (2019) 012038

doi:10.1088/1742-6596/1382/1/012038

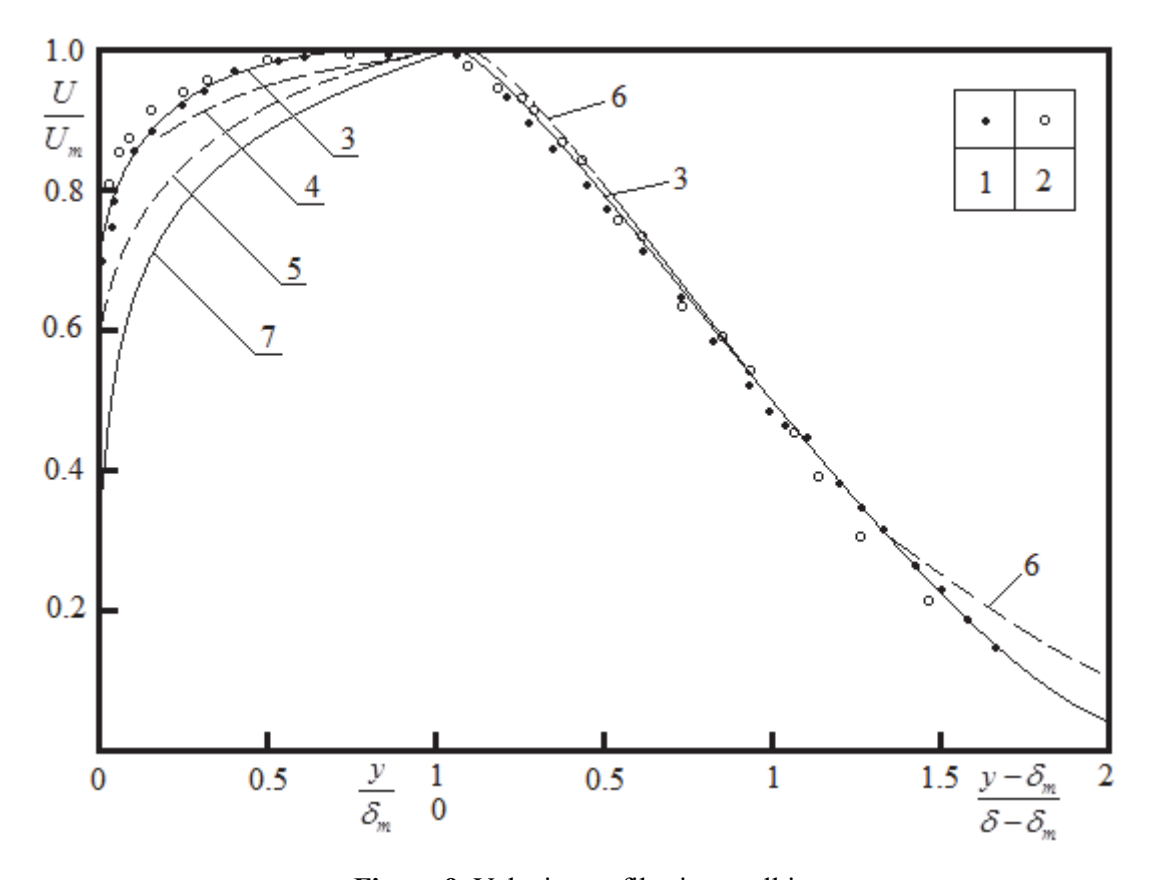


Figure 9. Velocity profiles in a wall jet

$$1 - \frac{x}{h} = 48.5$$
 (concave surface); $2 - \frac{x}{h} = 31.2$ (convex surface);

3 - Isataev formula (1);
$$4 - \frac{U}{U_m} = \left(\frac{y}{\delta_m}\right)^{1/12}$$
; $5 - \frac{U}{U_m} = \left(\frac{y}{\delta_m}\right)^{1/8}$; $6 - \frac{U}{U_m} = Ch^{-2}\left(0.882\frac{y - \delta_m}{\delta - \delta_m}\right)$; $7 - \frac{U}{U_m} = \left(\frac{y}{\delta_m}\right)^{1/5.5}$.

As it can be seen within the accuracy of the experimental data, the velocity profiles in the near-wall boundary layer are independent of both S_R parameter and its relative thickness of $\delta m/R$. However, works [4, 5] state that the velocity profiles in the near-wall boundary layer depend substantially on the streamlined surface curvature and become less filled on the convex surface and more filled on the concave surface. In these papers, velocity profiles are approximated as a power function.

$$\frac{U}{U_m} = \left(\frac{y}{\delta_m}\right)^{1/n} \tag{3}$$

where the exponent depends essentially on the relative thickness $\delta m/R$ and is determined by the following formula

$$\frac{n}{n_0} = 1 - 1.7 \left(\frac{\delta_m}{R}\right)^{0.31} \tag{4}$$

for a convex surface and

$$\frac{n}{n_0} = 1 + 269 \left(\frac{\delta_m}{R}\right)^{0.65} \tag{5}$$

for a concave surface.

1382 (2019) 012038 doi:10.1088/1742-6596/1382/1/012038

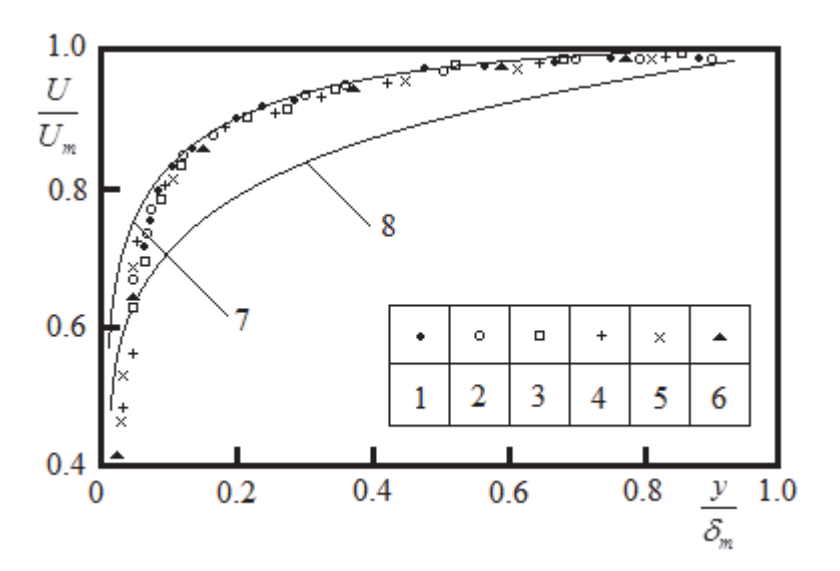


Figure 10. Wall layer profiles for jets on a concave surface

$$1 - \frac{x}{b} = 64, \ b = 5 \text{ mm}, \ \delta_m = 4.2; \ 2 - \frac{x}{b} = 98, \ b = 5 \text{ mm}, \ \delta_m = 5.0; \ 3 - \frac{x}{b} = 145, \ b = 5 \text{ mm}, \ \delta_m = 5.7;$$

$$4 - \frac{x}{b} = 21, \ b = 15 \text{ mm}, \ \delta_m = 4.5; \ 5 - \frac{x}{b} = 48.5, \ b = 15 \text{ mm}, \ \delta_m = 5.4; \ 6 - \frac{x}{b} = 32, \ b = 15 \text{ mm}, \ \delta_m = 5.0;$$

$$7 - \frac{U}{U_m} = 1.426 \left(\frac{y}{\delta_m}\right)^{1/8} \left(1 - 0.503 \frac{y}{\delta}\right)^{3/2}; \ 8 - \frac{U}{U_m} = \left(\frac{y}{\delta_m}\right)^{1/7}.$$

Here, n0 = 12 is the exponent corresponding to the velocity profile in the jet along a flat plate. According to their data at $\delta m/R = 0.02$ should be n = 14.6 - for a concave surface, and n = 5.5 - for a convex surface.

Figure 9 shows the calculated profiles corresponding to the formulas (3) and (4) with values n = 5.5; 8.0 and 12.0, as well as the profile for the outer part of the jet based on the following formula

$$\frac{U}{U_m} = ch^{-2} \left(0.882 \frac{y - \delta_m}{\delta - \delta_m} \right) \tag{6}$$

usually proposed for the free jet profile.

As it can be seen, in the near-wall region, formulas (4) and (5) [4, 5] are far apart with our data, which requires an explanation.

As it is known, it is almost impossible to measure velocity profiles very close to the wall using a hot-wire anemometer. Therefore, profiles in the wall boundary layer are measured by a Pitot tube with a flattened tip. The authors of these works, apparently, took measurements in the near-wall boundary layer with a total pressure Pitot tube. In the above works, experimental unit layouts do not provide for drain holes on the streamlined cylindrical surface for measuring static pressure near the cylinder surface. Apparently, the authors assumed that the static pressure near the walls was negligible compared to the dynamic pressure and its effect on the Pitot tube readings was neglected. As it can be seen from our data, the excess static pressure near the streamlined surface with a distance from the nozzle and an increase in the jet thickness can reach up to 30–40% of the velocity head corresponding to the maximum speed in this section. This can significantly distort the velocity measurement results.

1382 (2019) 012038 doi:10.1088/1742-6596/1382/1/012038

Conclusions

A wide range experimental study has been carried out with respect to jet aerodynamics distributing along the convex and concave cylindrical surfaces within a wide parameter range: initial curvature with parameters of curvature: $0 \le S_R = \frac{b}{R} \le |\pm 0.12|$, (signs "+" and "-"are referred to convex and concave surfaces, accordingly), nozzle thickness b=(5,0÷40,5) mm, initial jet velocity U_0 =(2,8÷56,0) m/s and acoustical effect frequency f=(108÷1344) Hz.

In all cases the jet distributing along convex and concave cylindrical surfaces did a U-turn at 180°.

It is established that in universal coordinates $\frac{U}{U^x} = f\left(\frac{yU^*}{v}\right)$ the wall-adjacent velocity profiles

demonstrate universal nature in the curvature parameter varying area: $0 \le S_R \le \left| \pm 0.12 \right|$, and actually coincide with the velocity profile of the turbulent boundary layer on a flat plate during homogeneous flowing around except for a pressure zone which is $10^4 \div 10^5$ times smaller than the lateral pressure gradient. As a result, the wall-adjacent velocity profile has much in common with the velocity profile on a flat plate with $\left| S_R \right| \le 0.12$. The statement of authors of widely known research papers [4,5] with regard to the curvature parameter with significant influence on the wall-adjacent velocity profile in a stream flowing along a curved surface within the above mentioned range of parameter curvature is proven unfounded.

It is established that in relative coordinates $\frac{U}{U_m} = f\left(\frac{y}{\delta}\right)$ the velocity profiles are affinely similar with accuracy ± 10 % across the entire jet area section.

It is established that maximum velocity reached along a convex surface becomes less whereas the jet span increases rapidly with a distance from the nozzle and as the curvature parameter grows rather than that of wall-adjacent jet along a flat plate. The reverse is true for the jet flowing along the concave surface. Based on review of experimental data, the semiempirical formulas were developed to calculate the jet maximum velocity and span in proportion to distancing from the nozzle and taking into account the curvature parameter.

References

- [1] Huang P G, Bradshaw P 1995 AIAA Journal 33 (4) 624–32
- [2] Gao D L, Chen W L, Li H Hu H 2017 Experimental Thermal and Fluid Science 82 287–301
- [3] Gao D, Chen G, Chen W, Huang Y, Li H 2019 Experimental Thermal and Fluid Science 102 575–88
- [4] Khalatov A A, Shevchuk I V, Avramenko A A 1992 Fluid Mechanics Research 21 (6) 29-51
- [5] Khalatov A A 1996 Inzhenerno-Fizicheskii Zhurnal 69 (6) 927–40
- [6] Gillis J C, Johnston J P 1983 Journal of Fluid Mechanics 135 123–53
- [7] Labusov A N, Lapin Yu V 2000 High Temperature **38** (3) 434–43
- [8] Mellor G L 1973 *Journal of Fluid Mechanics* **60** (1) 43–62
- [9] Ehirim O H, Knowles K, Saddington A J 2018 Journal of Fluids Engineering, Transaction of the ASME 141 (2) 020801
- [10] Yakirevich E, Miezner R, Leizeronok B, Gurkel B 2018 Journal of Engineering for Gas Turbines and Power 140 (1) 012301
- [11] Isataev S I, ToleuovG, Isataev M and Bolysbekova Sh A *Journal of Engineering Physics and Thermophysics* **89** (2) 391–6